Environmental Science & Technology

Article

pubs.acs.org/est

Modeling the Uptake of Semivolatile Organic Compounds by Passive Air Samplers: Importance of Mass Transfer Processes within the Porous Sampling Media

Xianming Zhang[†,‡] and Frank Wania*[,†,‡]

[†]Department of Chemistry, [‡]Department of Physical and Environmental Sciences, University of Toronto Scarborough, Toronto, Ontario M1C 1A4, Canada

Supporting Information

ABSTRACT: Air sampling based on diffusion of target molecules from the atmospheric gas phase to passive sampling media (PSMs) is currently modeled using the two-film approach. Originally developed to describe chemical exchange between air and water, it assumes a uniform chemical distribution in the bulk phases on either side of the interfacial films. Although such an assumption may be satisfied when modeling uptake in PSMs in which chemicals have high mobility, its validity is questionable for PSMs such as polyurethane foam disks and XAD-resin packed mesh cylinders. Mass transfer of chemicals through the PSMs may be subject to a large resistance because of the low mass fraction of gas-phase chemicals in the pores, where diffusion occurs. Here we present a model that does not assume that chemicals distribute uniformly in the PSMs. It describes the sequential diffusion of vapors through a stagnant air-side boundary layer and the PSM pores, and the reversible sorption onto the PSM. Sensitivity analyses reveal the potential influence of the latter two processes on passive sampling rates (PSRs) unless the air-side boundary layer is assumed to be extremely thick (i.e., representative of negligible wind speeds). The model also reveals that the temperature dependence of PSRs, differences in PSRs between different compounds, and a two-stage uptake, all observed in field calibrations, can be attributed to those mass transfer processes within the PSM. The kinetics of chemical sorption to the PSM from the gas phase in the macro-pores is a knowledge gap that needs to be addressed before the model can be applied to specific compounds.

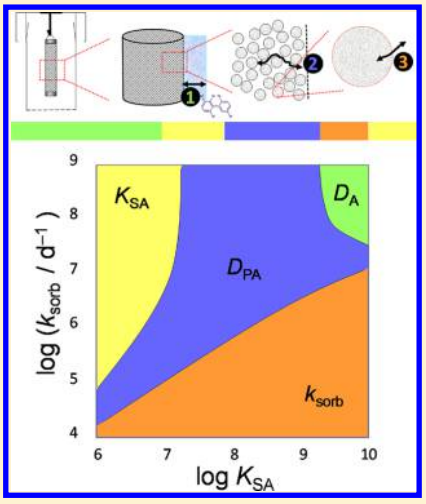

INTRODUCTION

Over the past decades, various types of passive air samplers (PASs) have been developed to monitor semivolatile organic compounds (SVOCs) in air.[1−4] Due to the advantages of low cost, simple and noise-free operation and no power requirement, applications of PASs range widely from investigating spatial and long-term temporal trends of SVOCs at local, regional and global scales[5−8] to identifying sources and assessing exposures of SVOCs in the air of various environments.[9−11]

Passive air sampling is based on molecular diffusion from the atmospheric gas phase to a passive sampling medium (PSM) such as polyethylene,[3] polymer-coated glass,[12] polyurethane foam (PUF),[1] and XAD-resin.[2] Unlike polyethylene or polymer-coated glass-based PAS, where SVOCs accumulate in thin layers in contact with air, the PSM in PUF and XAD-based PAS is relatively thick and porous. Chemical uptake by PSMs has been described using the two-film model,[13] which is often referred to as passive air sampling theory.[1,14,15] The two-film model was originally developed by Lewis and Whitman[13] to describe mass transfer between air and water. By replacing the water compartment with the PSM, the two-film model approach is applied to describe chemical transfer from air to the PSM. However, the two-film model requires that "*in the main body of either liquid or gas* [...] *the concentration of solute in the fluid is essentially uniform at all points.*"[13] While this assumption may be satisfied when modeling uptake in PSMs in which chemicals have high mobility, its validity is questionable for thick, porous PSMs such as PUF and XAD. Chemical transfer within such porous PSMs primarily occurs in the gas-filled pores, which limits the transfer kinetics because only a small mass fraction of the SVOCs may be in the porous gas phase within the PSM. Recently, a passive sampling experiment conducted using concentrically layered XAD and PUF indicated that SVOCs did not distribute uniformly within these PSMs over the exposure period (168 days for XAD or 84 days for PUF) but remained predominantly in outer layers in close contact with air.[16,17] Therefore, using the two-film approach and assuming uniform chemical distributions within the PSMs, the current PAS theory may not be able to fully describe the uptake of SVOCs from air to these bulk PSMs.

Received: March 17, 2012
Revised: July 27, 2012
Accepted: July 30, 2012
Published: July 30, 2012

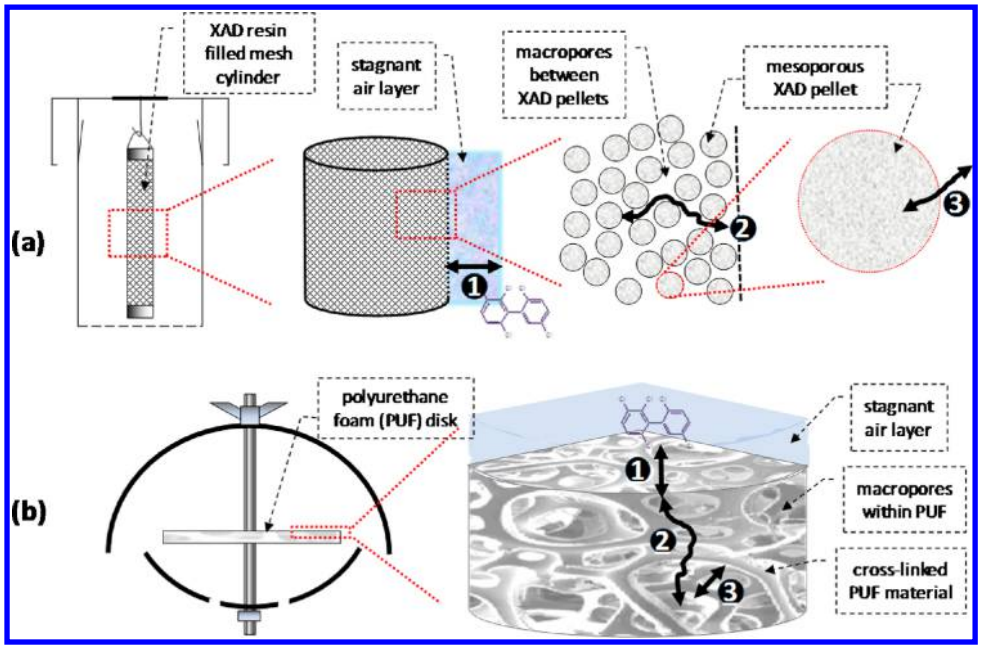

Figure 1. Conceptual diagram of the chemical mass transfer processes between air and the passive sampling media (PSMs) in the (a) XAD-resin based passive air sampler and (b) polyurethane foam based passive air sampler. The mass transfer processes include (1) diffusion through the stagnant air layer surrounding the PSM; (2) diffusion through macro-pores within the PSM; (3) sorption/desorption between porous air and solid PSM material. The microstructure of polyurethane foam was taken from a micrograph contributed by J. A. Elliott to the DoITPoMS Micrograph Library, University of Cambridge under the *Creative Commons Attribution Non-Commercial Share Alike* license.

If uptake in a PAS were indeed limited by the air side resistance only,[1,14,15] under a given wind condition or thickness of the stagnant air layer surrounding the PSM, a chemical's passive sampling rate (PSR) should be proportional to its diffusivity in air (D_A). According to the Fuller-Schettler-Giddings Equation,[18] D_A is a function of atmospheric pressure, temperature, and molecular size.[19,20] However, D_A is not sufficiently sensitive to these parameters to explain variations of PSR with temperature and differences in PSR between compounds/congeners observed in PAS calibration studies.[2,19−22] Whereas shifts in gas-particle partitioning[20] can to some extent explain PSR variations for SVOCs of very low volatility, they cannot serve as an explanation for the observed variations in the PSRs of most SVOCs, indicating that other factors must play a role. Furthermore, based on the two-film PAS theory,[1,14,15] the sampled amount (or equivalent air volume) increases linearly with time during the initial stage of chemical uptake by a PAS until uptake gradually slows due to re-evaporation from the PSM back to air. Deviating from this pattern, some recent calibration studies for PUF-PAS observed high PSRs initially followed by lower, yet relatively constant PSRs during later uptake.[23,24] Although these observations were conceptually described as a two-stage uptake mechanism,[23] no attempt was made to reconcile them with two-film PAS theory which fails to explain such behavior.

The objective of this study was to develop a model that does not require the assumption that chemicals distribute uniformly in the PSM but considers chemical diffusion through the stagnant air layer surrounding the PSM, diffusion through the air-filled pores within the PSM and sorption/desorption between the gas phase and the PSM material. The model is then applied to illustrate how the mass transfer processes and associated parameters affect the PSR.

MATERIALS AND METHODS

Conceptual Model of Chemical Mass Transfer during Passive Air Sampling. Currently, when describing the kinetics of SVOC uptake from air to PAS or the depuration from PSM to air, the PSM is treated as a bulk phase, in which chemical distribution is uniform and therefore no chemical mass transfer processes need to be considered.[1,2,14] Based on our previous experiments indicating the existence of a kinetic resistance to SVOC mass transfer within porous PSMs such as XAD resin and PUF,[16] we propose an alternative conceptual framework of a three-stage mass transfer process to describe sampling of SVOCs in PAS, which is illustrated in Figure 1. The first stage is the mass transfer of SVOCs through the stagnant air layer surrounding the bulk PSM (process 1 in Figure 1). This process is the same as that described by the two-film PAS theory.[1,14] After crossing the stagnant air layer, molecules can diffuse deeper into the PSM through macro-pores (process 2 in Figure 1). The terms "macro-pore" and "meso-pore" refer to pores with diameters of >50 nm and 2−50 nm, respectively.[25] Simultaneously, molecules can sorb to the solid PSM material (process 3 in Figure 1). As XAD pellets have meso-pores ~9 nm in diameter,[26] the molecules will not only adsorb to the outer pellet surface, but will also diffuse through the meso-pores and sorb to sites deeper within the XAD pellets. Therefore, process 3 for the XAD-PAS involves both meso-pore diffusion and sorption/desorption.

Adsorption is generally believed to be the primary process for the retention of chemicals in polymers at temperatures below their glassy state transition temperature (T_g).[28] The T_g of XAD is above 100 °C,[27] which suggests that adsorption is dominant at environmentally relevant temperatures. However, according to the dual-mode sorption theory, dissolution (partition) of the chemical into the polymer could also occur at temperatures below T_g.[29] Even though the contribution of partition/absorption relative to adsorption is likely to be very small, we

do not distinguish "adsorption" and "absorption" but describe the uptake of chemical from air to XAD using the general term "sorption".

Mathematical Model of Chemical Mass Transfer During Passive Air Sampling. To quantitatively describe (i) molecular diffusion through the stagnant air layer surrounding the PSM, (ii) diffusion though the macro-pores within the PSM and (iii) sorption/desorption between gas-filled macro-pores and solid PSM material, we applied (i) Fick's law, (ii) the diffusion-reaction equation based on Fick's law and the principles of mass conservation, and (iii) the law of mass action. Due to the different geometries of XAD-filled mesh cylinders and PUF disks (Figure 1), Fick's law of diffusion in cylindrical coordinates and in a plane was applied to XAD-PAS and PUF-PAS, respectively. The model for the XAD-PAS is presented below; the one for the PUF-PAS is described in the Supporting Information (SI).

Diffusion Across the Stagnant Air Layer. Close to the interface between air and the bulk PSM, eddies become diminished owing to the viscous nature of air and the air flow rate decreases drastically because of frictional forces.[30] As a result, a stagnant air layer (air-side boundary layer) is formed at the interface. Chemical mass transfer through this layer is attributed to molecular diffusion, which can be described by Fick's law:[31]

$$\frac{\partial C_A(r,t)}{\partial t} = D_A\frac{\partial^2 C_A}{\partial r^2} + D_A\frac{1}{r}\frac{\partial C_A}{\partial r},\ r_S < r < r_S + \delta_{BL} \tag{1}$$

where C_A (ng/cm^3) is the vapor concentration in air at position r (cm) at PAS deployment time t (d); r is the position on the radial coordinate originating in the center of the XAD-filled mesh cylinder (SI Figure S1); r_S (cm) is the radius of this cylinder and δ_{BL} (cm) is the thickness of the stagnant air layer. D_A (cm^2/d) is the molecular diffusivity in bulk air.

Diffusion within the Porous PSM. Within the PSM, it is assumed diffusion along the radial coordinate only occurs in the air-filled macro-pores (i.e., negligible diffusion through solid phase). Different from diffusion in bulk air, diffusion in porous media is retarded due to the more tortuous path and reduced area for diffusion.[32] Thus, diffusivity in the porous air phase (D_{PA}, cm^2/d) is related to the diffusivity in bulk air and the void fraction (ε, unitless) of the PSM:[32]

$$D_{PA} = D_A\cdot\varepsilon^{4/3} \tag{2}$$

The behavior of molecules in the macro-pores is not only related to diffusion, but also affected by the kinetics of reversible sorption of the vapor in the macro-pores to the XAD pellets. A mass balance equation for molecules in the macro-pores subject to these two processes is

$$\frac{\partial C_A(r,t)}{\partial t} = D_{PA}\frac{\partial^2 C_A}{\partial r^2} + D_{PA}\frac{1}{r}\frac{\partial C_A}{\partial r} - \rho\frac{\partial C_S}{\partial t},\ 0 < r < r_S \tag{3}$$

where C_A (ng/cm^3) is the concentration in the air-filled macro-pores, ρ (g/cm^3) is the density of bulk XAD, and C_S (ng/g) is the mass concentration in the XAD pellets.

Chemical Exchange between Air-filled Macro-pores and XAD Pellets can be represented by the following chemical equation:[30]

$$M + S \rightleftharpoons M\cdots S \tag{4}$$

where M represents the gas phase molecule in the macro-pores, S represents the polymeric sorbent, and $M\cdots S$ represents the sorbed molecule. Due to the large amount of meso-pores within XAD, the sites available for sorption can be assumed to be constant and eq 4 can be simplified to[33]

$$M \underset{k_{des}}{\overset{k_{sorb}}{\rightleftharpoons}} M\cdots S \tag{5}$$

where k_{sorb} (d^{-1}) and k_{des} (d^{-1}) are the sorption and desorption rate constants, respectively. k_{sorb} and k_{des} are related to the equilibrium partition coefficient between the sorbent and air ($K_{SA} = k_{sorb}/k_{des}$). Note that sorption/desorption as used here comprises also molecular diffusion through the meso-pores within the XAD pellets. In principle, such meso-pore diffusion could be described with an additional diffusion equation of spherical coordinates.[34,35] The size of individual XAD pellets is much smaller than that of the XAD-filled mesh cylinder. During passive air sampling, the diffusion path through the bulk XAD-filled mesh cylinder is much longer than the intraparticle diffusion path. Thus, intraparticle diffusion should have a trivial effect on the overall mass transfer kinetics. Furthermore, due to the lack of information on chemical transfer within XAD pellets, for the purpose of this study, the kinetics of mass transfer processes within XAD pellets were integrated into k_{sorb} and k_{des}. Similar approaches have been adopted to model sorption of chemicals to sorbents such as activated carbons and sediments.[33,36] Applying the law of mass action to the pseudo first order reaction (eq 5),[33,37] the mass balance of chemical sorbed to the PSM can be quantified by

$$\frac{\partial C_S(r,t)}{\partial t} = \frac{k_{sorb}C_A}{\rho} - k_{des}C_S,\ 0 < r < r_S \tag{6}$$

Model Solution. By replacing the spatial derivatives with finite differences (200 nodes in the PSM and 50 nodes in the stagnant air layer, which is illustrated in SI Figures S1 and S2), the partial differential equations (eqs 1, 3, and 6) become a system of ordinary differential equations (details in the SI), which can be solved numerically under the initial (t = 0) and boundary/interfacial (r = 0; $r = r_S$; $r = r_S + \delta_{BL}$) conditions described in the SI. The model outputs chemical concentrations in the stagnant air layer, in the macro-porous air phase and in the PSM as a function of space and time. By spatially integrating the concentrations, the amount accumulated in the PSM at any time point can be derived. Following the practice of PAS field calibrations,[20] in which a PSR is often derived as the slope of the linear regression between the equivalent air volume and the length of deployment, we calculated model-derived PSRs by selecting six equally spaced time points from zero to the maximum deployment time and applying a linear fit (forced through the origin) with the corresponding equivalent sampling volumes retrieved from the model output (example in SI Figure S3). Note that these model-derived PSRs are not the same as the theoretical ("intrinsic") PSRs defined in Bartkow et al.,[14] which are presumed constant for a given set of conditions (e.g., diffusivity in air, boundary layer thickness, temperature). In fact, the instantaneous PSR is always changing, even during the so-called linear uptake phase.

Sensitivity Analysis. To investigate which of the three chemical mass transfer processes involved in passive air sampling is more influential on the PSR (m^3/d), we performed a sensitivity analysis on the PSR (90 days deployment time) by varying by ±10% one of the parameters (δ_{BL}, D_A, D_{PA}, K_{SA}, and k_{sorb}) governing the three mass transfer processes. Note that although D_A, D_{PA}, and K_{SA} are correlated (SI Figure S5), we

dx.doi.org/10.1021/es302334r | Environ. Sci. Technol. 2012, 46, 9563−9570

only varied one parameter at a time in order to reveal the influential processes and parameters. Sensitivity coefficients (SC) were calculated as $SC = (\Delta y/y)/(\Delta x/x) = [(y_+ - y_-)/(y_+ + y_-)]/[(x_+ - x_-)/(x_+ + x_-)]$, in which x and y are the model input and output, respectively, and the subscripts $_+$ and $_-$ designate values with the model input parameters increased and decreased by 10%, respectively. Because the influence of a model parameter on model results is often dependent on the value of that and other parameters, we conducted a global sensitivity analysis considering combinations of the parameters varying over a wide, but reasonable range. $K_{XAD/A}$ and $K_{PUF/A}$ for specific chemicals have been well established.[38,39] The ranges selected for $K_{XAD/A}$ ($10^6 \le K_{XAD/A} \le 10^{10}$) and $K_{PUF/A}$ ($10^5 \le K_{PUF/A} \le 10^9$) cover most SVOCs (on average, $K_{XAD/A}$ are larger than $K_{PUF/A}$ by $\sim 10^{0.8}$; SI Figure S4).[16,39] The ranges of D_A and D_{PA} are determined by the K_{SA} range due to the correlation between these parameters (SI Figure S5 and eq 2). A previous study established that the thickness of the air boundary layer surrounding a cylinder of 2 cm diameter ranged between 0.1 and 0.01 cm under wind speeds between 1 and 10 m/s.[40] Since wind speeds can exceed 10 m/s, we selected 0.01 cm as the base case for δ_{BL} and investigated the δ_{BL} range between 0.001 and 0.1 cm. Because no empirical information on likely values of k_{sorb} for sorption of SVOCs onto XAD or PUF existed, we chose a range of k_{sorb} values ($10^4\ d^{-1} \le k_{sorb} \le 10^9\ d^{-1}$) for which the model yields PSRs that match the range of those measured in calibration studies. k_{sorb} values reported for the sorption of VOCs onto activated carbon also fall within this range.[36]

Model Application. The model described above was applied to investigate the variation of PSRs with chemical properties and temperatures. Such variations observed in field PAS calibrations[2,19,20] are larger than can be explained by the two-film PAS model,[1,14] which presumes that temperature influences PSRs only via the influence on D_A. In the model presented, PSR is a function of D_A, D_{PA}, K_{SA}, k_{sorb}, and k_{des}. These parameters vary between different chemicals and are temperature dependent. The temperature dependence of D_A and D_{PA} is quantified by the Fuller-Schettler-Giddings equation[18] and the dependence of K_{SA} can be quantified with the van't Hoff equation using a measured or predicted internal energy of sorption (ΔU_{SA}).[38,39] The temperature dependence of k_{sorb} and k_{des} can be described with the Arrhenius equation:

$$k_{sorb} = A_1 \exp(-E_{a+}/RT) \quad (7a)$$

$$k_{des} = A_2 \exp(-E_{a-}/RT) \quad (7b)$$

where A_1 and A_2 are pre-exponential factors, E_{a+} and E_{a-} are the activation energies of the forward and backward reactions in eq 5, R is the ideal gas constant, and T is absolute temperature (K). E_+, E_- and ΔU_{SA} are interrelated (illustrated in SI Figure S6) through

$$\Delta U_{SA} = E_{a+} - E_{a-} \quad (8)$$

Using the model, we also investigated the chemical uptake curve with the intention of explaining a rapid decrease in the PSR of the PUF-PAS after the first few weeks of sampling.[23,41] Lastly, with the model, we calculated the penetration depths of chemicals in the PSM. Because there is a lack of information on k_{sorb} or k_{des} (and the parameters in eqs 7 and 8) for specific chemicals, model calculations were performed on a range of values.

RESULTS AND DISCUSSION

Influence of Mass Transfer Processes and Associated Parameters on the Passive Air Sampling Rate. The sensitivity analysis reveals how the chemical mass transfer through the stagnant air layer surrounding the PSM (δ_{BL}, D_A), the diffusive mass transfer in the macro-pores within the PSM (D_{PA}), and the reversible sorption from the gas phase to the PSM (K_{SA} and k_{sorb}) influence the PSR. The sensitivity of the PSR to model parameters was calculated and displayed in the coordinate system defined by K_{SA} and k_{sorb} (referred to as sensitivity map hereafter) at different δ_{BL} (Figure 2 and SI Figure S7). Based on the sensitivity (SC > 0.5) of the parameters, the sensitivity map could generally be divided into four regions (shown in Figure 2f) for both XAD-PAS and PUF-PAS for different assumed values of δ_{BL}.

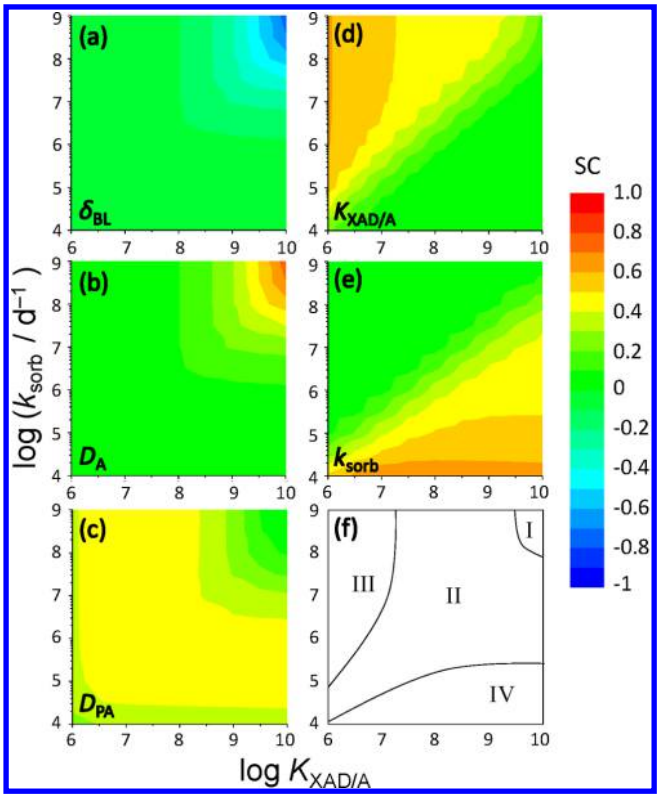

Figure 2. Sensitivity (SC) of the sampling rate (PSR, m^3/d) of the XAD-based passive air sampler for compounds with different equilibrium partition coefficients between XAD and air ($K_{XAD/A}$) and different sorption rate constants (k_{sorb}) to changes in (a) the thickness of the stagnant air layer (δ_{BL}), (b) the molecular diffusivity in bulk air (D_A), (c) the molecular diffusivity in the macroporous fraction within the XAD (D_{PA}), (d) $K_{XAD/A}$, and (e) k_{sorb}. δ_{BL} = 0.01 cm was used as the baseline for the SC calculations. Based on the other five panels, panel (f) identifies four regions, in which the PSR is predominantly influenced by a particular mass transfer process.

In region I, PSRs are most sensitive to δ_{BL} and D_A (Figures 2a and b). δ_{BL} and D_A together determine the mass transfer coefficient in the stagnant air layer ($k_A = D_A/\delta_{BL}$), which explains why the effects of δ_{BL} and D_A on PSR are equal in magnitude but reverse in direction. In other words, PSR would increase (decrease) equally either by increasing (decreasing) D_A or decreasing (increasing) δ_{BL} to the same extent. Therefore, hereafter we focus only on D_A in our analysis of mass transfer within the stagnant air layer. In this region, the kinetics of the

dx.doi.org/10.1021/es302334r | Environ. Sci. Technol. 2012, 46, 9563−9570

overall mass transfer is limited by the chemical diffusion through the stagnant air layer surrounding the PSM. Moving from region I to region II, PSRs become less sensitive to D_A and more sensitive to D_{PA} (Figure 2c), indicating that the chemical mass transfer through the macro-pores within the PSM becomes more influential on the PSRs. Chemicals in region I have high K_{SA} and k_{sorb} relative to those in region II. The PSM has a high capacity for such chemicals, which therefore are more likely to sorb to the outer layer of the PSM than to penetrate to the inside. Thus, D_{PA} is less influential on the PSR of chemicals in region I than of those in region II.

In region III, PSRs are most sensitive to a chemical's K_{SA} or the uptake capacity of the PSM (Figure 2d). Chemicals in this region have relatively low K_{SA} and high k_{sorb}. The low PSM capacities for the chemicals and the fast rates of sorption/desorption to the PSM allow surface evaporation to play an important role in chemical mass transfer between air and the PSM. Lowering the K_{SA} increases the rate of chemical evaporation from the PSM and thus reduces the PSR during the deployment period. In region IV, PSRs are most sensitive to k_{sorb}. The reason is that in this region, k_{sorb} is low and the overall rate of mass transfer from ambient air to the PSM is kinetically limited by the rate of sorption from the gas phase in the macro-pores to the solid PSM material. In both regions III and IV, PSRs are also sensitive to D_{PA} (Figure 2c). In region III, an increased D_{PA} facilitates penetration into the PSM, which competes with the surface evaporation process that cause chemical loss from the PSM. In region IV, while the PSRs are limited by the sorption kinetics, an increased D_{PA} makes more of the sorbent deep inside the PSM accessible for sorption, and thus increases the PSRs.

The boundaries between the four regions shift on the sensitivity map when the thickness of the stagnant air layer (δ_{BL}) is changed due to, for example, a change in wind conditions (SI Figure S7). The thicker the stagnant air layer, the larger the number of chemicals whose overall mass transfer is controlled by the diffusion across the stagnant air layer. Thus, when δ_{BL} increases, the sensitivity of PSRs to D_A or δ_{BL} increases and the boundary between region I and II shifts toward the center of map. As the kinetic resistance to diffusion through the stagnant air layer increases with increasing δ_{BL}, so does the kinetic resistance to evaporation from the PSM. This decreases the influence of surface evaporation on the PSRs for chemicals for which this process is important (i.e., chemicals with low K_{SA}). Therefore, region III shifts toward lower K_{SA} with increased δ_{BL}. As the kinetics for chemical crossing the stagnant air layer becomes more influential to the overall uptake, the sorption rate would have to be lower in order to kinetically limit the overall uptake process. Thus, region IV shifts toward lower k_{sorb} as δ_{BL} increases.

Comparing the sensitivity maps based on the models for XAD-PAS and PUF-PAS (SI Figure S7), region I for the PUF-PAS extends to lower K_{SA} and lower k_{sorb} than for the XAD-PAS, indicating that the stagnant air layer resistance (D_A/δ_{BL}) is more important in determining the PSR in PUF-PAS than in XAD-PAS. This difference could be due to differences in the configuration (cylindrical XAD-resin filled mesh cylinder vs planar PUF sheet) and/or physical properties (density and macro-pore fraction) of the PSM. To investigate the contributions of these two factors, we conducted a sensitivity analysis using models in which the cylindrical XAD-filled mesh cylinder in the XAD-PAS model was replaced by a cylindrical PUF of the same dimension or the PUF disk in the PUF-PAS model was changed to an XAD disk. The sensitivity maps based on the modified models (SI Figure S8) indicate that it is the density and porosity (SI Table S1) of the PSMs rather than their geometrical arrangement that explains the difference in the importance of the stagnant boundary layer.

A specific chemical with known K_{SA} and k_{sorb} is represented by a point on the sensitivity maps. K_{SA}s for both XAD and PUF have been well characterized and are generally positively correlated with molecular size. So far, information on the rates of sorption and desorption (i.e., k_{sorb} and k_{des}) to PSM is lacking. However, based on the theory of mass transfer between a fluid and a single spherical particle,[42] k_{sorb} is positively correlated with the molecular diffusivity in the fluid and thus negatively correlated with the molecular volume. Therefore, K_{SA} is presumably negatively correlated with k_{sorb}. As such, points representing real chemicals on the sensitivity map are more likely to distribute within a belt from the top left to the bottom right and the likelihoods for a chemical to have both high (low) K_{SA} and high (low) k_{sorb} (i.e., distributed in the upper right and lower left region of the map) are low.

Influence of Chemical Properties and Temperatures on Passive Air Sampling Rates. In order to explain the variation of PSRs with temperature and between different compounds, we constructed a chemical space map displaying the PSR calculated for different combinations of K_{SA} and k_{sorb}. As an illustration, the chemical space map showing the PSR for uptake in an XAD-PAS deployed for 360 d assuming δ_{BL} = 0.01 cm is shown in Figure 3. A color scale represents the PSR with

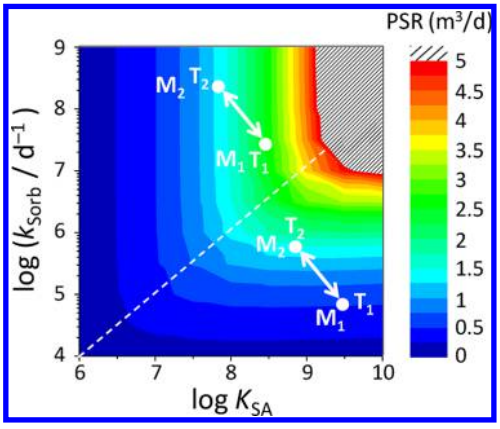

Figure 3. Illustration of the dependence of passive sampling rates (PSRs) on chemical properties and temperature. Molecular size: $M_1 > M_2$; temperature $T_1 < T_2$. The map depicting PSRs in the K_{SA}-k_{sorb} chemical space was constructed based on the model for a XAD-passive air sampler deployed for 360 days assuming a stagnant air boundary layer thickness δ_{BL} of 0.01 cm. PSRs exceeding 5 m^3/d were calculated for the combination of large K_{SA} and large k_{sorb} (hatched area), which is unlikely to exist among real chemicals.

changes in K_{SA} and k_{sorb}. Maps with lower and higher wind exposure of the XAD-PAS (δ_{BL} = 0.1 and 0.001 cm) are presented in SI Figure S9. Recall that K_{SA} is correlated with D_A and D_{PA} (SI Figure S5) and thus the maps integrate the variation of D_A and D_{PA} with K_{SA}. The maps display L-shaped strips of different colors, each representing a range of PSRs. The dashed line connecting the inflection points of all the L-shaped strips divides the map into two regions. On the upper-left (lower-right) region, the strips are generally parallel with the y-axis (x-axis), indicating PSRs for chemicals in this region are sensitive to changes in K_{SA} (k_{sorb}) but not sensitive to the

dx.doi.org/10.1021/es302334r | Environ. Sci. Technol. 2012, 46, 9563−9570

changes in k_{sorb} (K_{SA}). This pattern of PSRs in the chemical space map agrees with the results of the sensitivity analysis (Figure 2d and e).

The hatched area on the top right of the map represents a PSR above 5 m^3/d, which has rarely been observed in a field calibration using the XAD-PAS. As mentioned before, K_{SA} is generally negatively correlated with k_{sorb}; smaller chemicals in a homologous series tend to have a low K_{SA} and a high k_{sorb}. Therefore, points representing a homologous series on the map would distribute along a line from the bottom right to the top left and a point representing a chemical on the chemical space map would shift toward the upper left (lower right) at higher (lower) temperatures. As indicated by the model results, different chemicals or a chemical at different temperatures would be expected to have different PSRs. Depending on the chemical properties (K_{SA} and k_{sorb}), the direction in which the PSR changes with chemical properties and temperatures can be different. For chemicals in the lower right of the map (high K_{SA} and low k_{sorb}), the PSR for a homologous series decreases with increasing molecular size ($M_1 > M_2$ in Figure 3). In contrast, if the sorption of the chemicals to the sorbent is fast (k_{sorb} is large) so that the chemicals are positioned on the upper left, a chemical with large molecular size (M_1) would have a higher PSR than a smaller chemical (M_2). Similarly, the variation of the PSR with temperature can be different depending on a chemical's K_{SA} and k_{sorb}, i.e. its position in the map. PSRs for chemicals positioned in the lower right (upper left) increase (decrease) as temperature increases (from T_1 to T_2 as illustrated in Figure 3).

The model facilitates a mechanistic explanation of this seemingly contradictory behavior. The PSR of chemicals in the lower right is kinetically controlled by the sorption process and the diffusion within the PSM. As K_{SA} decreases and k_{sorb} increases with a decrease in molecular size or an increase in temperature, the fraction in the air-filled pores increases, facilitating the penetration into the PSM. The increased diffusivity within the PSM and the increased sorption rate (k_{sorb}) will increase the PSR. For chemicals in the upper left region, k_{sorb} is large so that chemicals accumulate rapidly at the PSM surface. Increased chemical accumulation at the surface with increased k_{sorb} and the decreased sorbent capacity (K_{SA}) would enhance the role that surface evaporation plays in decreasing the PSR.

Many studies on passive air sampling have observed the variation of PSRs among different chemicals or for a chemical at different temperatures.[2,19−21] For the XAD-PAS, PSRs were found to be positively correlated with D_A but the variation in PSR was much larger than that of D_A.[2,19] For the PUF-PAS, the relationship between PSRs and D_A seems more complicated. Some studies observed a negative correlation of PSRs with D_A: higher PSRs for chemicals at lower temperatures and for highly chlorinated biphenyls.[20,21] On the contrary, lower PSRs for highly brominated diphenyl ethers have also been observed.[41] One explanation for the variation of PSRs in PUF-PAS is a shift in the gas-particle distribution of the target SVOCs:[20] at lower (higher) temperature or for a heavier (lighter) congener, a higher (lower) fraction of the chemicals would be in the particle phase so the amount of chemicals in the gas phase available for uptake decreases (increases). Considering a lower sampling efficiency for particle-bound chemicals than for chemicals in the gas phase, PSR calibrated against bulk air concentrations becomes lower (higher). Although this process could possibly affect the PSR of SVOCs with very low volatility (e.g., highly brominated diphenyl ethers), it cannot explain the PSR variation for chemicals predominantly in gas phase (e.g., tri- and tetra-chlorinated biphenyls). Comparing the field observations with the map in Figure 3, it seems that a model that considers the kinetic resistance within the PSM can explain the observed PSR variations for both XAD-PAS and PUF-PAS. The observed behavior of the XAD-PAS agrees with the case on the bottom right of the map (higher K_{SA} and lower k_{sorb}) and that of the PUF-PAS follows that in the upper left region (lower K_{SA} and higher k_{sorb}). While K_{SA} for XAD has been found to be generally higher than that for PUF, no information on k_{sorb} for XAD or PUF is currently available. Because sorption to XAD involves diffusion through the meso-pores within each pellet, which may limit the sorption kinetics, k_{sorb} for XAD is presumably lower than for PUF.

Two-Stage Uptake Process. In the PUF-PAS calibration studies by Chaemfa et al.[23] and by Tsurukawa et al.,[24] some chemicals are observed to have a high PSR initially (~1−2 weeks) after which the PSR drops and stays relatively constant. A two-stage uptake was hypothesized to explain such an observation but no quantitative studies were conducted and no mechanistic explanation was formulated. We used the model to construct the uptake curves for chemicals with different combinations of K_{SA} and k_{sorb} (SI Figure S10). Two-stage uptake was predicted for chemicals with high k_{sorb}. Sorption of such chemicals to the surface of the PSM is faster than diffusive penetration into the PSM. Initially, sorption occurs at the surface of the PSM, the resistance to diffusion in the PSM pores is not rate-controlling, and the PSR is determined by the fast sorption rate. As the PSM surface becomes saturated, the chemical either evaporates or diffuses into the PSM. The overall uptake kinetics is then determined by the rate of diffusion into the PSM, which leads to a decreased PSR compared with the initial uptake phase. Although the model can mechanistically explain a two-stage uptake, we are unable to use the model to predict the uptake for specific compounds due to the lack of information on k_{sorb}.

Non-Uniform Chemical Distribution within Passive Sampling Media. The model describing the mass transfer processes within PSMs is capable of calculating the radial distribution of chemicals within the PSM. Agreeing with experimental evidence,[16] the model calculations for the K_{SA}−k_{sorb} chemical space indicate a nonuniform chemical distribution within the PSMs. For the majority of K_{SA} and k_{sorb} combinations, a surface layer of less than 0.4 cm thickness contains >90% of the amount of chemical accumulated in the PSM of both XAD- and PUF-PAS after 90 days of deployment (SI Figure S11). Our experiments investigating chemical distribution within the PSMs were based on cylindrical PSM configurations.[16] The mass transfer of chemicals within such cylindrical PSMs might be retarded as the cross-sectional area for diffusion decreases from the outer to the inner part of the PSM. This could possibly add some uncertainty when extrapolating the experimental results based on PSMs of cylindrical configuration to those of planar configuration (disk). Model calculations for PSMs in both cylindrical and planar configurations (SI Figure S11) revealed no obvious differences in the penetration depth (defined as the thickness of the outer PSM layer which accumulates 90% of the sampled amount). This indicates that the nonuniform distribution within the PSM is mainly determined by the competition between sorption and diffusion deeper into the PSM rather than the PSM configuration.

Knowledge Gap and Implications. In this study, the new model was primarily used to provide mechanistic insight into some field observations that could not be explained with the two-film PAS theory. The new model's capability to describe the behavior of specific chemicals is mainly limited by the lack of quantitative information on k_{sorb}, either from measurements or predictions. Unlike other model parameters such as D_A, D_{PA}, and K_{SA}, which either have been measured or can be predicted with established theories for SVOCs,[30,38,39] k_{sorb} has only been studied for the sorption of some VOCs (e.g., benzene, carbon tetrachloride) on a few sorbents other than XAD or PUF.[36,43] In order to quantitatively describe specific chemicals and to expand the application of the model, k_{sorb} and its temperature dependence need to be quantified for SVOCs and the PSMs commonly used in PASs. Once k_{sorb} is available for specific chemicals, this model could be used to predict chemical specific PSRs at different temperatures. The model results on the chemical distribution within the PSMs could also be useful when optimizing the design of PASs with the intention of improving the sampling efficiency. For example, increasing the interfacial area/volume ratio of a PSM would prevent the sorbent in the inner part of the PSM from being wasted.

In field applications of PASs, PSRs are often determined from calibrations against active air samplers instead of being calculated from PAS theory. Therefore, although both experimental[16] and modeling evidence (this study) indicates nonuniform chemical distribution within porous PSMs, which contradicts the assumption in the two-film approach, interpretation of PAS data using empirically derived PSRs will not be affected, as long as PSRs are used that are compound- and sampling site specific. The two-film PAS theory has previously been used to estimate linear uptake ranges[1,20,39] or to calculate PSRs from the observed loss of depuration compounds.[44] By neglecting to consider the kinetic resistance within the PSM, linear uptake ranges tend to be overestimated because deeper parts of the PSM are not readily accessible. This agrees with observed linear uptake ranges that are shorter than estimated for heavier compounds that do not penetrate readily into the PSMs.[44] PSRs, through their dependence on K_{SA} and k_{sorb}, are clearly compound-specific, and the applicability of a PSR obtained for one type of (depuration) compound to another cannot be assumed but would need to be demonstrated. Even if depuration compounds are isotopically labeled analogs of the target compounds, PSRs derived from the loss of depuration compounds (without accounting for a kinetic resistance within the PSM) may deviate from the PSRs of chemicals sampled from air because their distributions within the PSM are different and thus result in different kinetic resistances within the PSM.

■ ASSOCIATED CONTENT

Supporting Information

Further information on the model development and additional modeling results. This material is available free of charge via the Internet at http://pubs.acs.org.

■ AUTHOR INFORMATION

Corresponding Author

*Phone: +1-416-287-7225; e-mail: frank.wania@utoronto.ca.

Notes

The authors declare no competing financial interest.

■ ACKNOWLEDGMENTS

We acknowledge research funding from the Canadian Foundation for Climate and Atmospheric Sciences and the Natural Sciences and Engineering Research Council of Canada. X.Z. acknowledges financial support from an Ontario Graduate Scholarship.

■ REFERENCES

(1) Shoeib, M.; Harner, T. Characterization and comparison of three passive air samplers for persistent organic pollutants. *Environ. Sci. Technol.* **2002**, *36*, 4142−4151.

(2) Wania, F.; Shen, L.; Lei, Y. D.; Teixeira, C.; Muir, D. C. G. Development and calibration of a resin-based passive sampling system for monitoring persistent organic pollutants in the atmosphere. *Environ. Sci. Technol.* **2003**, *37*, 1352−1359.

(3) Bartkow, M. E.; Hawker, D. W.; Kennedy, K. E.; Müller, J. F. Characterizing uptake kinetics of PAHs from the air using polyethylene-based passive air samplers of multiple surface area-to-volume ratios. *Environ. Sci. Technol.* **2004**, *38*, 2701−2706.

(4) Farrar, N. J.; Harner, T.; Shoeib, M.; Sweetman, A.; Jones, K. C. Field deployment of thin film passive air samplers for persistent organic pollutants: A study in the urban atmospheric boundary layer. *Environ. Sci. Technol.* **2005**, *39*, 42−48.

(5) Shen, L.; Wania, F.; Lei, Y. D.; Teixeira, C.; Muir, D. C. G.; Bidleman, T. F. Atmospheric distribution and long-range transport behavior of organochlorine pesticides in North America. *Environ. Sci. Technol.* **2005**, *39*, 409−420.

(6) Shunthirasingham, C.; Oyiliagu, C. E.; Cao, X. S.; Gouin, T.; Wania, F.; Lee, S. C.; Pozo, K.; Harner, T.; Muir, D. C. G. Spatial and temporal pattern of pesticides in the global atmosphere. *J. Environ. Monit.* **2010**, *12*, 1650−1657.

(7) Schuster, J. K.; Gioia, R.; Harner, T.; Lee, S. C.; Breivik, K.; Jones, K. C. Assessment of sorbent impregnated PUF disks (SIPs) for long-term sampling of legacy POPs. *J. Environ. Monit.* **2012**, *14*, 71−78.

(8) Schuster, J. K.; Gioia, R.; Breivik, K.; Steinnes, E.; Scheringer, M.; Jones, K. C. Trends in European background air reflect reductions in primary emissions of PCBs and PBDEs. *Environ. Sci. Technol.* **2010**, *44*, 6760−6766.

(9) Bohlin, P.; Jones, K. C.; Levin, J. O.; Lindahl, R.; Strandberg, B. Field evaluation of a passive personal air sampler for screening of PAH exposure in workplaces. *J. Environ. Monit.* **2010**, *12*, 1437−1444.

(10) Cheng, Y.; Shoeib, M.; Ahrens, L.; Harner, T.; Ma, J. M. Wastewater treatment plants and landfills emit volatile methyl siloxanes (VMSs) to the atmosphere: Investigations using a new passive air sampler. *Environ. Pollut.* **2011**, *159*, 2380−2386.

(11) Zhang, X. M.; Diamond, M. L.; Robson, M.; Harrad, S. Sources, emissions, and fate of polybrominated diphenyl ethers and polychlorinated biphenyls indoors in Toronto, Canada. *Environ. Sci. Technol.* **2011**, *45*, 3268−3274.

(12) Farrar, N. J.; Harner, T. J.; Sweetman, A. J.; Jones, K. C. Field calibration of rapidly equilibrating thin-film passive air samplers and their potential application for low-volume air sampling studies. *Environ. Sci. Technol.* **2005**, *39*, 261−267.

(13) Lewis, W. K.; Whitman, W. G. Principles of gas absorption. *Ind. Eng. Chem.* **1924**, *16*, 1215−1220.

(14) Bartkow, M. E.; Booij, K.; Kennedy, K. E.; Müller, J. F.; Hawker, D. W. Passive air sampling theory for semivolatile organic compounds. *Chemosphere* **2005**, *60*, 170−176.

(15) Tuduri, L.; Millet, M.; Briand, O.; Montury, M. Passive air sampling of semi-volatile organic compounds. *TrAC, Trends Anal. Chem.* **2012**, *31*, 38−49.

(16) Zhang, X. M.; Tsurukawa, M.; Nakano, T.; Lei, Y. D.; Wania, F. Sampling medium side resistance to uptake of semi-volatile organic compounds in passive air samplers. *Environ. Sci. Technol.* **2011**, *45*, 10509−10515.

(17) Zhang, X. M.; Wong, C.; Lei, Y. D.; Wania, F. Influence of sampler configuration on the uptake kinetics of a passive air sampler. *Environ. Sci. Technol.* **2012**, *46*, 397−403.

(18) Fuller, E. N.; Schettler, P. D.; Giddings, J. C. A new method for prediction of binary gas-phase diffusion coefficients. *Ind. Eng. Chem.* **1966**, *58*, 18−27.
(19) Gouin, T.; Wania, F.; Ruepert, C.; Castillo, L. E. Field testing passive air samplers for current use pesticides in a tropical environment. *Environ. Sci. Technol.* **2008**, *42*, 6625−6630.
(20) Melymuk, L.; Robson, M.; Helm, P. A.; Diamond, M. L. Evaluation of passive air sampler calibrations: Selection of sampling rates and implications for the measurement of persistent organic pollutants in air. *Atmos. Environ.* **2011**, *45*, 1867−1875.
(21) Klánová, J.; Èupr, P.; Kohoutek, J.; Harner, T. Assessing the influence of meteorological parameters on the performance of polyurethane foam-based passive air samplers. *Environ. Sci. Technol.* **2008**, *42*, 550−555.
(22) Hazrati, S.; Harrad, S. Calibration of polyurethane foam (PUF) disk passive air samplers for quantitative measurement of polychlorinated biphenyls (PCBs) and polybrominated diphenyl ethers (PBDEs): Factors influencing sampling rates. *Chemosphere* **2007**, *67*, 448−455.
(23) Chaemfa, C.; Barber, J. L.; Gocht, T.; Harner, T.; Holoubek, I.; Klanova, J.; Jones, K. C. Field calibration of polyurethane foam (PUF) disk passive air samplers for PCBs and OC pesticides. *Environ. Pollut.* **2008**, *156*, 1290−1297.
(24) Tsurukawa, M.; Suzuki, M.; Okuno, T.; Takemine, S.; Okada, Y.; Matsumura, C.; Nakano, T. Calibration and field survey of passive air samplers for persistent organic pollutants. *Organohalogen Compd.* **2010**, *72*, 884−887.
(25) Sing, K. S. W.; Everett, D. H.; Haul, R. A. W.; Moscou, L.; Pierotti, R. A.; Rouquerol, J.; Siemieniewska, T. Physisorption data for gas solid systems with special reference to the determination of surface-area and porosity. *Pure Appl. Chem.* **1985**, *57*, 603−619.
(26) Sigma-Aldrich. Amberlite XAD-2 polymeric adsorbent product specification. http://www.sigmaaldrich.com/etc/medialib/docs/supelco/product_information_sheet/4802.par (accessed January 2012).
(27) Nakagawa, H.; Tsuge, S. Characterization of styrene divinylbenzene copolymers by high-resolution pyrolysis-gas chromatography. *Macromolecules* **1985**, *18*, 2068−2072.
(28) Courval, G.; Gray, D. G. Effect of surface adsorption on gas-chromatographic measurements near polymer melting transitions. *Macromolecules* **1975**, *8*, 326−331.
(29) Panda, S.; Bu, Q.; Huang, B.; Edwards, R. R.; Liao, Q.; Yun, K. S.; Parcher, J. F. Mass spectrometric inverse gas chromatography: Investigation of polymeric phase transitions. *Anal. Chem.* **1997**, *69*, 2485−2495.
(30) Schwarzenbach, R. P.; Gschwend, P. M.; Imboden, D. M. *Environmental Organic Chemistry*, 2nd ed.; Wiley: Hoboken, NJ, 2003.
(31) Louch, D.; Motlagh, S.; Pawliszyn, J. Organic-compound extraction from water using liquid-coated fused-silica fibers. *Anal. Chem.* **1992**, *64*, 1187−1199.
(32) Mackay, D. *Multimedia Environmental Models: The Fugacity Approach*, 2nd ed.; Lewis Publishers: Boca Raton, 2001.
(33) Harper, M. P.; Davison, W.; Tych, W. DIFS - a modelling and simulation tool for DGT induced trace metal remobilisation in sediments and soils. *Environ. Model. Software* **2000**, *15*, 55−66.
(34) Ruthven, D. M. *Principles of Adsorption and Adsorption Processes*; Wiley: New York, 1984.
(35) Katsanos, N. A.; Bakaoukas, N.; Koliadima, A.; Karaiskakis, G.; Jannussis, A. Diffusion and adsorption measurements in porous solids by inverse gas chromatography. *J. Phys. Chem. B* **2005**, *109*, 11240−11246.
(36) Chuang, C. L.; Chiang, P. C.; Chang, E. E. Modeling VOCs adsorption onto activated carbon. *Chemosphere* **2003**, *53*, 17−27.
(37) Tovbin, Y. K. Chapter 4. Theory of adsorption-desorption kinetics on flat heterogeneous surfaces. In *Stud. Surf. Sci. Catal.*, Rudziński, W.; Steele, W. A.; Zgrablich, G., Eds. Elsevier: 1997; Vol. *104*, pp 201−284.
(38) Kamprad, I.; Goss, K. U. Systematic investigation of the sorption properties of polyurethane foams for organic vapors. *Anal. Chem.* **2007**, *79*, 4222−4227.
(39) Hayward, S. J.; Lei, Y. D.; Wania, F. Sorption of a diverse set of organic chemical vapors onto XAD-2 resin: Measurement, prediction and implications for air sampling. *Atmos. Environ.* **2011**, *45*, 296−302.
(40) Nobel, P. S. Boundary-layers of air adjacent to cylinders - estimation of effective thickness and measurements on plant material. *Plant Physiol.* **1974**, *54*, 177−181.
(41) Chaemfa, C.; Barber, J. L.; Moeckel, C.; Gocht, T.; Harner, T.; Holoubek, I.; Klanova, J.; Jones, K. C. Field calibration of polyurethane foam disk passive air samplers for PBDEs. *J. Environ. Monit.* **2009**, *11*, 1859−1865.
(42) Suzuki, M. *Adsorption Engineering*; Kodansha; Elsevier: Tokyo, 1990.
(43) Ribeiro, A. M.; Sauer, T. P.; Grande, C. A.; Moreira, R. F. P. M.; Loureiro, J. M.; Rodrigues, A. E. Adsorption equilibrium and kinetics of water vapor on different adsorbents. *Ind. Eng. Chem. Res.* **2008**, *47*, 7019−7026.
(44) Moeckel, C.; Harner, T.; Nizzetto, L.; Strandberg, B.; Lindroth, A.; Jones, K. C. Use of depuration compounds in passive air samplers: Results from active sampling-supported field deployment, potential uses, and recommendations. *Environ. Sci. Technol.* **2009**, *43*, 3227−3232.